Anal Bioanal Chem
DOI 10.1007/s00216-016-9869-1

RESEARCH PAPER

Development of a novel ultrasonic-assisted magnetic dispersive solid-phase microextraction method coupled with high performance liquid chromatography for determination of mirtazapine and its metabolites in human urine and water samples employing experimental design

Mahdi Ghorbani[1] · Mahmoud Chamsaz[1] · Gholam Hossein Rounaghi[1] · Mohsen Aghamohammadhasani[2] · Orkideh Seyedin[2] · Nahid Afshar Lahoori[2]

Received: 22 May 2016 / Revised: 28 July 2016 / Accepted: 9 August 2016
© Springer-Verlag Berlin Heidelberg 2016

Abstract Ultrasonic-assisted magnetic dispersive solid-phase microextraction coupled with high performance liquid chromatography has been developed for extraction and determination of mirtazapine, *N*-desmethyl mirtazapine, and 8-hydroxy mirtazapine in human urine and water samples. Magnetic graphene oxide–polyaniline nanocomposite (MGOPA) as a novel SPME sorbent was synthesized and used for the microextraction process. The analytical performance of MGOPA was compared with magnetic graphene oxide nanocomposite and indicated that the new sorbent was quite effective for extraction of mirtazapine, *N*-desmethyl mirtazapine, and 8-hydroxy mirtazapine. A two-stage experimental design approach, Plackett-Burman screening design and Box-Behnken optimization design, was used for screening and optimizing of significant variables in the microextraction process. The practical applicability of the proposed method was assessed by studying the linearity, intra-day and inter-day accuracy, enrichment factor, and precision. This method can be satisfactorily applied to the determination of mirtazapine and its metabolites in human urine and environmental water samples.

Keywords Graphene oxide nanocomposite · Mirtazapine · Dispersive solid-phase microextraction · Plackett-Burman design · Box-Behnken design · High performance liquid chromatography

Electronic supplementary material The online version of this article (doi:10.1007/s00216-016-9869-1) contains supplementary material, which is available to authorized users.

✉ Mahmoud Chamsaz
mchamsaz@gmail.com

[1] Department of Chemistry, Faculty of Sciences, Ferdowsi University of Mashhad, Mashhad, Iran

[2] Department of Chemistry, Mashhad Branch, Islamic Azad University, Mashhad, Iran

Introduction

Pharmaceuticals are widely used to treat human and animal diseases. After drugs are taken, they are absorbed and metabolized in human and animal bodies. These drugs and their metabolites are finally excreted to the sewage system by the kidneys. Therefore, these compounds are known as a source of environmental contamination when they get into the environmental water samples. When antidepressant drugs and their active metabolites are released into environmental water samples, they have undesirable effects on the organs of animals and humans, such as change in behavior and reproduction in fish [1, 2]. Moreover, the drugs are accumulated in fish and subsequently enter into the human body through the contaminated food. Therefore, a new trend in analytical chemistry is vital to determine these contaminants in real water samples with high accuracy, selectivity, and sensitivity because their concentrations are very low in environmental matrices [3, 4].

Mirtazapine (MRT) is a tetracyclic antidepressant that is used for the treatment of depression with noradrenergic and specific serotonergic activity. It is also commonly used to treat anxiety, insomnia, loss of appetite, and nausea [5, 6]. MRT is mainly metabolized by the cytochrome P450 enzyme system in the liver to *N*-desmethyl mirtazapine (DMR) and 8-hydroxy mirtazapine (8-OHM). Metabolites of MRT have no therapeutic effects and almost all orally administered doses are

Published online: 25 August 2016

excreted via urine and feces within 4 d [6–8]. Chemical structures of MRT and its metabolites are shown in Electronic Supplementary Material (ESM) Fig. S1.

Sample preparation is a major stage in determining analyte in real sample prior to analysis. The proper choice of sample preparation methodology has a great effect in drug analysis because analyte is converted into a suitable form for measurement step and matrix effects and interfering species are also decreased with these techniques. Solid phase microextraction (SPME) has been widely applied as a unique sample preparation technique for extraction of drugs from biological and water samples utilizing some advantages such as being solvent-free, simple, and cost-effective [9–14]. We have recently introduced a new approach of SPME [4] called ultrasonic-assisted magnetic dispersive solid-phase microextraction (UAMDSPME), which is a combination of ultrasonic enhanced dispersive liquid–liquid microextraction (UADLLME) and magnetic solid-phase microextraction (MSPME). UAMDSPME has several advantages, such as low extraction time, simple operation, cost effectiveness, is rapid, organic solvent free, has high preconcentration factor, low sorbent consumption, and variety in the choice of sorbent.

One of the carbon allotropes is graphene oxide (GO), which is widely used as SPME sorbent. The chief advantages of GO as sorbent are large specific surface area, high adsorption capacity, and simple and inexpensive preparation method. Owing to nanoscale morphology and low thickness of GO sheet, its surface area and the number of suitable interaction sites of GO sheet is higher than conventional SPME sorbent. Moreover, extraction efficiency of analyte using GO sheet is higher than conventional SPME sorbent. The presence of oxygen-containing functional groups in the graphene oxide surface with a noncovalent interaction such as hydrogen bonding and van der Waals interaction cause good solubility and dispersion of GO into water and numerous solvents [15]. Moreover, these functional groups in the GO surface can easily be modified with other functional groups and materials to increase the extraction efficiency and selectivity in SPME [15–17].

A simple and fast method for preconcentration and determination of mirtazapine and its metabolites in human urine and environmental water samples was developed based on ultrasonic-assisted magnetic dispersive solid-phase microextraction (UADSPME) coupled with HPLC technique. In order to obtain suitable selectivity and efficiency of microextraction method, magnetic graphene oxide–polyaniline nanocomposite (MGOPA) was prepared and applied as a novel SPME sorbent. The optimal experimental conditions of the proposed microextraction procedure were studied with a two-step design of experiment stratagy(DOE)-based Plackett-Burman (P-B) screening design and Box-Behnken optimization design (B-B). In order to investigate the analytical performance of the new SPME sorbent, MGOPA was compared with magnetic graphene oxide nanocomposite for extraction of MRT, DMR, and 8-OHM.

Experimental

Reagents and materials

MRT, DMR, and 8-OHM of pharmaceutical quality were kindly supplied by Organon (Oss, The Netherlands). One thousand μg mL^{-1} standard solutions of mirtazapine, *N*-desmethyl mirtazapine, and 8-hydroxy mirtazapine in methanol were prepared and stored at 4 °C before use. HPLC grade acetonitrile and methanol were purchased from Merck (Darmstadt, Germany). All other materials used to prepare magnetic graphene oxide–polyaniline nanocomposite were of analytical grade and obtained from Merck (Darmstadt, Germany).

Instruments

A Knauer HPLC (Knauer Associates, Germany) equipped with a port sample injection valve (7725i; Reodyne, Cotati, CA, USA) with a 20 μL injection loop, a UV detector (K-2600) was used for determination of MRT, DMR, and 8-OHM. The chromatographic separation was carried out at room temperature (22 ± 0.5 °C) on a Shim-Pack VP-ODS C18 column (4.6 mm × 250 mm, 5.0 μm). The mobile phase, acetonitrile-phosphoric acid/potassium dihydrogen phosphate buffer (pH 3) (30:70, v/v) was delivered at a flow rate of 1.5 mL/min. The UV detector was set at the wavelength of 294 nm. The pH of the solution was adjusted by Metrohm 691 pH meter. In order to disperse magnetic graphene oxide–polyaniline nanocomposite into the sample solution, a compact ultrasonic Hiescher up 100 h (100 W, 30 kHz) was used.

Synthesis of graphene oxide–polyaniline nanocomposite

Graphene oxide nanosheets (GO) was prepared according to the previous article [18]. Twenty-three mL of concentrated H_2SO_4 (23 mL) was added to a mixture containing 0.5 g of graphite flakes and 0.5 g of $NaNO_3$ while the mixture was slowly stirred and cooled down to 0 °C in an ice bath. $KMnO_4$ (3.0 g) was gradually added to the suspension and the temperature of the mixture was kept lower than 20 °C. The suspension was ultrasonically treated for 20 min at room temperature and followed by adding 40 mL of deionized water. In order to reduce the $KMnO_4$ residual, a solution containing 3 mL H_2O_2 (30 %) in 100 mL deionized water was gradually added to the resulting suspension until the solution color changed from dark brown to yellow. The resulting product (GO) was collected by filtration and washed three times with 5 % HCl solution to remove any metal ion impurities and sulfate ions. In order to remove the excess acid, GO was finally rinsed with distilled water and dried under vacuum at 80 °C for 24 h.

In order to convert hydroxyl, ester, and epoxide groups to carboxylic functional groups, a mixture of NaOH (0.4 g) and

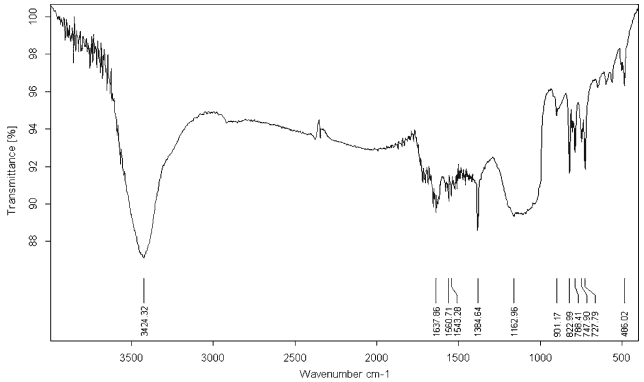

Fig. 1 FT-IR spectrum of graphene oxide–polyaniline nanocomposite

$ClCH_2COONa$ (0.4 mg) was added to the GO suspension (0.3 g) in distilled water (3 mL) and treated in ultrasonic bath for 2 h at room temperature. The suspension (carboxyl-functionalized graphene oxide, CFGO) was then neutralized by dilute hydrochloric acid and centrifuged until the product was well-dispersed in deionized water [19].

For synthesis of graphene oxide–polyaniline (GO–PANI), 60 mg CFGO in 30 mL distilled water was dispersed by sonication for 5 min and 2.76 mL of aniline in 1.0 mol L^{-1} HCl was added to it. The suspension was ultrasonically treated for 1 h at room temperature. A solution of ammonium per sulfate (1.71 mg) in 1.0 mol L^{-1} HCl was then added dropwise to the suspension and placed in ultrasonic bath for 2 h. After filtration, the resulting product was washed with deionized water, ethanol, and hexane and dried at 50 °C in vacuum for 24 h [20].

Synthesis of magnetic graphene oxide–polyaniline nanocomposite by co-precipitation

GO–PANI (0.3 g) in 150 mL distilled water was dispersed by sonication for 30 min, and the solution of $FeCl_3 \cdot 6H_2O$ (0.825 g) and $FeCl_2 \cdot 4H_2O$ (0.322 g) in 25 mL of distilled water was added to it with vigorous stirring at room temperature under the nitrogen flow. The pH of mixture was raised to 10 by dropwise addition of ammonia solution (28 %) until a black precipitate was formed after stirring for about 45 min. The black precipitate was washed with ethanol several times, and finally dried at 50 °C in vacuum [21]. The FTIR spectrum and SEM image of GO–PANI are shown in Figs. 1 and 2, respectively.

Ultrasonic-assisted magnetic dispersive solid-phase microextraction

A solution of 14.5 mL of MRT, DMR, and 8-OHM was placed in a 20 mL conical test tube. In order to adjust the pH of sample solution at 7.1, sodium dihydrogen phosphate/disodium hydrogen phosphate buffer was added (sample solution No 1).

Twenty mg of MGOPA was poured into a conical test tube followed by triton X100 (10 μL) and deionized water (1 mL). In order to disperse MGOPA, the mixture was ultrasonically treated for 3 min. The resulting suspension was rapidly injected into the MRT and its metabolites standard solutions (sample solution No 1) by an auto sampler, followed by shaking for 30 s. MGOPA particles were dispersed in the sample solution and a cloudy mixture was rapidly formed. MRT, DMR, and 8-OHM were then extracted on the surface of these fine particles. MGOPA was then separated from the sample solution under a strong external magnetic field and the supernatant solution was discarded. The absorbed analytes were ultrasonically eluted from the surface of MGOPA by 1.0 mL of methanol for 162 s, and 20 μL of the acceptor phase was accurately injected into the chromatographic system for analysis.

Calculation of extraction recovery and preconcentration factor

In order to obtain the optimized extraction, the percentage of extraction recovery, ER%, was used and calculated using the following equation:

$$ER\% = \left(C_{\text{acceptor phase}} \times V_{\text{acceptor phase}} / C_{\text{donor phase}} \times V_{\text{donor phase}}\right) \times 100$$

where $C_{\text{acceptor phase}}$ and $C_{\text{donor phase}}$ are the concentration of the analyte in the methanol phase and the water sample,

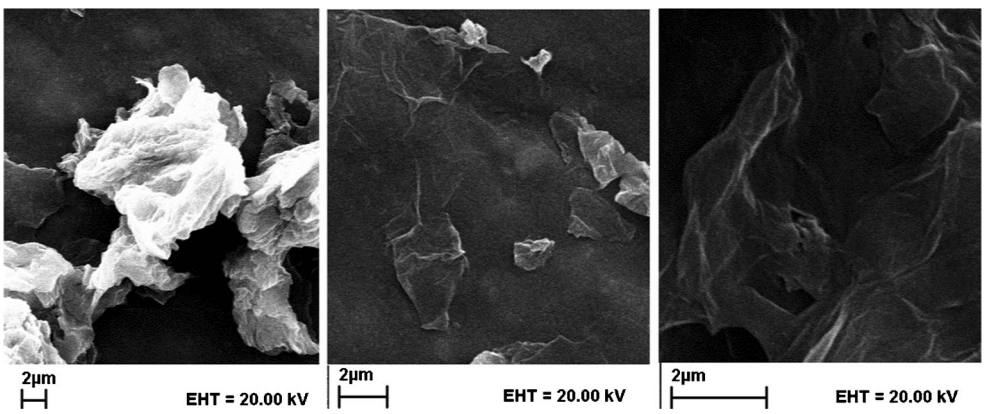

Fig. 2 SEM image of graphene oxide–polyaniline nanocomposite

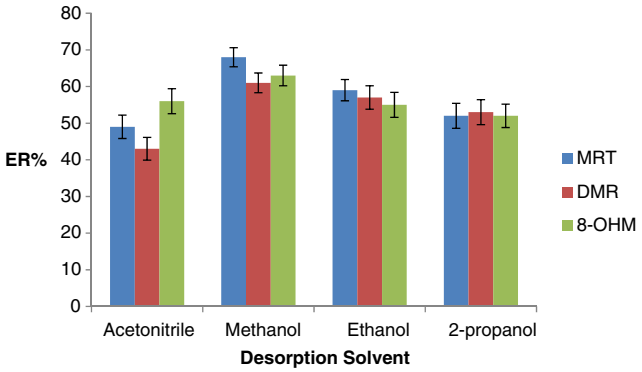

Fig. 3 Effect of type of desorption solvent on the extraction

respectively. $V_{acceptor\ phase}$ and $V_{donor\ phase}$ are volumes of the methanol and water sample, respectively.

Preconcentration factor (PF) defined as the ratio of the concentrations of analyte in the methanol phase and the initial concentration of the analyte in the water sample solution was calculated based on the following equation:

$$PF = C_{acceptor\ phase}/C_{donor\ phase}$$

$C_{donor\ phase}$ and $C_{acceptor\ phase}$ were practically determined from the calibration curves using direct injection of analyte standard solutions before the extraction and methanol phase injection after the extraction, respectively.

Results and discussion

Optimization of the microextraction procedure

In order to obtain higher selectivity, sensitivity, and precision for extraction of MRT and its metabolites with the UADSPME method, the effect of main parameters, such as pH of sample solution, donor phase volume, surfactant volume (triton X100), extraction time, dispersing time, desorption time, desorption solvent volume, type of desorption solvent, amount of sorbent, amount of salt, and shaking rate were thoroughly optimized. Type of desorption solvent is an effective parameter in extraction recovery because the absorbed analyte must be ultrasonically eluted from the surface of MGOPA with a suitable solvent prior to the

Table 1 Factors, codes, levels in the Plackett-Burman design matrix

Factors	Levels		
	Low (−1)	Center (0)	High (+1)
(F_1) pH of sample solution	3	6	9
(F_2) Amount of triton x-100 (mL)	10	35	50
(F_3) Dispersing time(min)	2	5	8
(F_4) Donor phase volume (mL)	5	12.5	20
(F_5) Desorption time(s)	100	150	200
(F_6) Extraction time (s)	10	20	30
(F_7) Amount of sorbent (mg)	10	15	20
(F_8) Desorption solvent volume (mL)	0.5	1	1.5
(F_9) Shaking rate (rpm)	400	650	900

Runs	F_1	F_2	F_3	F_4	F_5	F_6	F_7	F_8	F_9	ER % for MRT	ER % for DMR	ER % for 8-OHM
1	–1	–1	–1	–1	–1	–1	–1	–1	–1	29.8	27.8	31.3
2	0	0	0	0	0	0	0	0	0	92.1	93.8	92.8
3	1	1	–1	1	–1	–1	–1	1	1	71.4	69.2	77.2
4	1	1	1	–1	1	1	–1	1	–1	75.8	68.4	75.6
5	0	0	0	0	0	0	0	0	0	90.7	92.8	93.2
6	0	0	0	0	0	0	0	0	0	93.4	93.1	93.7
7	1	–1	1	1	–1	1	–1	–1	–1	75.9	73.5	77.1
8	1	1	–1	1	1	–1	1	–1	–1	88.1	84.6	89.9
9	–1	1	–1	–1	–1	1	1	1	–1	37.6	41.9	29.8
10	–1	–1	1	1	1	–1	1	1	–1	53.4	53.1	51.2
11	1	–1	–1	–1	1	1	1	–1	1	79.2	83.9	81.3
12	–1	1	1	1	–1	1	1	–1	1	49.7	56.4	59.1
13	–1	1	1	–1	1	–1	–1	–1	1	46.3	51.6	57.8
14	–1	–1	–1	1	1	1	–1	1	1	75.2	76.9	79.4
15	1	–1	1	–1	–1	–1	1	1	1	67.7	71.1	71.5

analysis. Hence, the extraction recovery is increased by increasing the desorption efficiency. On this basis, ethanol, methanol, 2-propanol, and acetonitrile were evaluated as desorption solvents. According Fig. 3, methanol gave the highest ER% and it was chosen as desorption solvent for extraction of MRT, DMR, and 8-OHM.

In order to optimize the parameters affecting the proposed microextraction procedure, the effects of the main parameters were investigated using chemometric approach based on the Plackett-Burman (P-B) screening design and the Box-Behnken optimization design (B-B). MINITAB version14 software was applied for the experimental design generations and study of the experimental data.

Screening design

An experimental P-B design was used to screen the significant factors affecting the microextraction efficiency. The preliminary experiments show that nine factors may be effective in the proposed microextraction (ESM Table S1). Therefore, a P-B design was created to screen the significant factors. This design showed 15 experiments, including 12 runs and three center points, and randomly performed to remove the uncontrolled variable effects [22, 23]. The level of each factor and its symbol is shown in Table 1. These levels were determined on the basis of preliminary experiments. Each experiment was repeated three times and the mean extraction recovery was calculated and used as a response. The responses were evaluated by analysis of variance with a 95 % probability. According to ANOVA Table, the factor is considered to be statistically significant at 95 % confidence level when its *p*-value is less than 0.05 in the Table. Pareto chart can also be used for evaluating the importance of the main factors. By plotting all the experimental results on a Pareto chart, it is easier to view and compare the main effects of all components. Therefore, the effect of factor in the ER% is more impressive by increasing the bar length on the plot. Moreover, the factor is considered to be statistically significant when the bar length of factor passes form reference line (t-value) on the chart. The effects of the studied factors in the ER% of the screening design are shown in a Pareto chart for each analyte (Fig. 4). The results indicate that three factors, the pH of sample solution, desorption time, and donor phase volume, were the significant variables for extraction of all analytes. Shaking rate was the other significant variable for extraction of DMR and 8-OHM but was not a significant variable in the extraction of MRT. Therefore, four variables (the pH of sample solution, desorption time, donor phase volume, and shaking rate) were selected to evaluate the optimization of design step. The pH had the most significant effect on the extraction efficiency and the other three factors, desorption time,

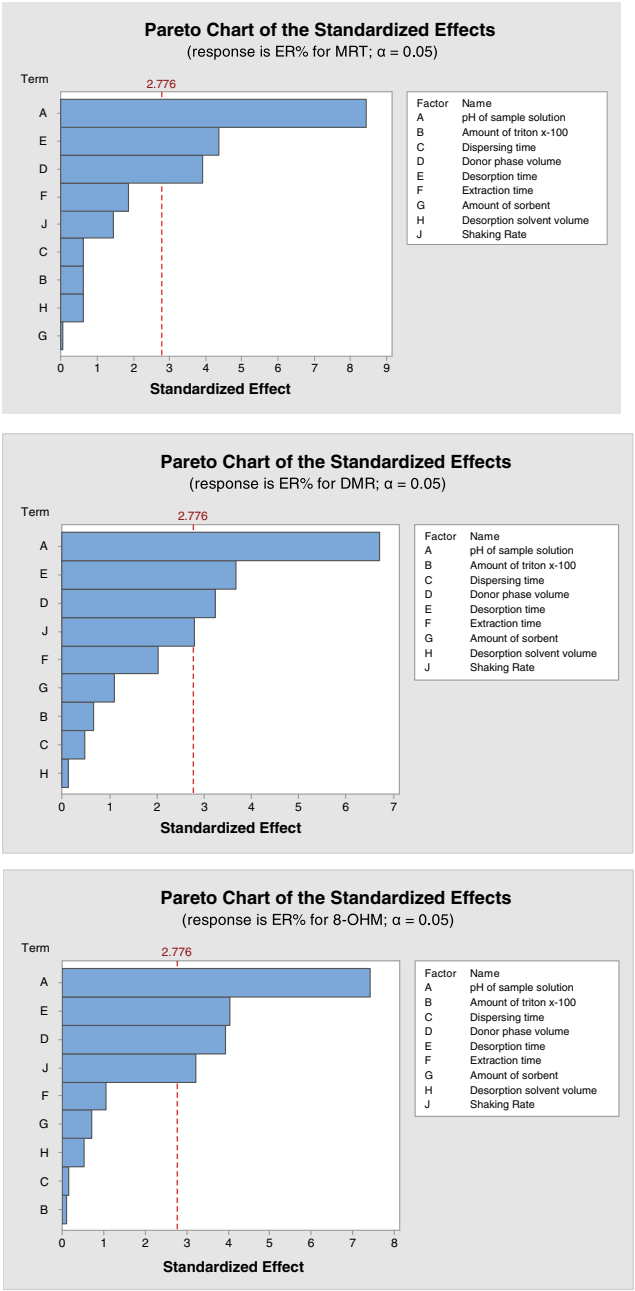

Fig. 4 Standardized main effect Pareto charts for the Plackett—Burman design for MRT, DMR, and 8-OHM. Vertical line in the chart defines 95 % confidence level

donor phase volume, and shaking rate, had the next most important significant effects on the ER%, respectively. All significant variables have positive effects on the ER% of all analytes. Comparison between the four significant factors show that pH is much more effective than the other three factors, but the effects of the other three factors on the ER% are much closer. Other not significant variables, including desorption solvent volume, amounts of triton X100, extraction time, dispersing time, and amounts of sorbent were fixed at 1.0 mL, 10 μL, 30 s, 3 min, and 20 mg, respectively.

Optimization design

Response surface design is applied to optimize the significant factors in experimental design and derived into two main type designs, Box-Behnken (B-B design) and central composite (C-C design). The main advantage of the B-B design over the C-C design is the lower number of runs for three and four factors [24]. In order to optimize the four factors selected from the first screening P-B design, a Box-Behnken design including 27 experiments, 24 runs, and three center points, was developed. The levels of each factor and matrix of B-B design are shown in Table 2. Analysis of variance was performed to study the results at 95 % confidence level ($p < 0.05$). A full qudratic model can be used to fit the response with the main factors, interaction between same and different main factors effect by the B-B design, which can be expressed according to the following equation:

$$ER\% = \beta_0 + \beta_1 F_1 + \beta_4 F_4 + \beta_5 F_5 + \beta_9 F_9 + \beta_{11} {F_1}^2 + \beta_{44} {F_4}^2 + \beta_{55} {F_5}^2 + \beta_{99} {F_9}^2 + \beta_{14} F_1 F_4 + \beta_{15} F_1 F_5 + \beta_{19} F_1 F_9 + \beta_{45} F_4 F_5 + \beta_{49} F_4 F_9 + \beta_{59} F_5 F_9$$

where β_0 is the intercept, β_1 to β_{59} represent the regression coefficients (uncoded units). The equation regression coefficients for each analyte and standard error of coefficients are listed in Table 3.

Table 2 Factors, codes, levels in the Box-Bohnken design matrix

Factors	Levels						
	Low (−1)			Center (0)		High (+1)	
(F_1) pH of sample solution	5			0		9	
(F_4) Donor phase volume (mL)	5			12.5		20	
(F_5) Desorption time(sec)	100			150		200	
(F_9) Shaking rate (rpm)	500			650		800	
Runs	F_1	F_4	F_5	F_9	ER % for MRT	ER % for DMR	ER % for 8-OHM
1	1	0	0	–1	76.3	78.0	76.5
2	0	1	1	0	87.3	93.2	86.5
3	1	0	1	0	82.6	81.1	78.6
4	–1	0	0	1	81.2	83.4	80.5
5	0	–1	0	1	88.7	89.5	84.3
6	0	0	–1	–1	79.8	85.6	81.9
0	0	0	–1	1	86.2	88.9	86.4
8	0	0	1	1	88.6	87.9	86.4
9	0	–1	1	0	89.1	89.7	85.2
10	–1	–1	0	0	86.9	84.8	82.1
11	–1	0	–1	0	77.2	75.8	74.9
12	1	1	0	0	86.5	87.7	80.4
13	0	–1	0	–1	88.9	86.3	85.8
14	0	1	0	–1	86.4	88.5	84.5
15	0	0	0	0	91.6	91.7	91.1
16	–1	1	0	0	73.3	76.4	75.5
10	–1	0	1	0	83.9	84.5	79.3
18	0	–1	–1	0	86.5	85.3	80.3
19	1	–1	0	0	72.8	68.2	66.8
20	0	0	0	0	93.5	92.4	89.3
21	0	0	0	0	91.9	91.3	90.7
22	–1	0	0	–1	77.8	78.0	74.1
23	0	0	1	–1	85.4	88.3	83.5
24	0	1	–1	0	86.4	88.9	87.7
25	1	0	–1	0	79.4	78.9	75.9
26	0	1	0	1	89.0	91.7	87.1
27	1	0	0	1	80.7	79.6	74.6

Table 3 Estimated parameters of the polynomial model for extraction of MRT, DMR, and 8-OHD

Term	MRT			DMR			8-OHD		
	Coded units		Uncoded units	Coded unit		Uncoded units	Coded units		Uncoded units
	Coef[a]	SE Coef[b]	Coef	Coef	SE Coef	Coef	Coef	SE Coef	Coef
Constant	0.973	94.86	–107.1	0.905	101.47	–104.3	1.00	90.41	–146.5
F1	–0.167	0.487	28.99	–0.783	0.452	35.13	–1.133	0.500	39.09
F4	–0.333	0.487	–2.658	1.883	0.452	–2.416	1.433	0.500	–0.951
F5	1.783	0.487	0.539	1.775	0.452	0.418	1.033	0.500	0.453
F9	1.650	0.487	0.2106	1.358	0.452	0.1573	1.083	0.500	0.2121
F1*F1	–9.712	0.730	–2.428	–10.525	0.679	–2.631	–11.067	0.750	–2.767
F4*F4	–1.812	0.730	–0.0322	–1.300	0.679	–0.0231	–2.692	0.750	0.0479
F5*F5	–2.988	0.730	–0.0012	–1.563	0.679	–0.000625	–2.642	0.750	0.001057
F9*F9	–3.413	0.730	0.00015	–1.863	0.679	0.000083	–2.767	0.750	–0.000123
F1*F4	6.825	0.843	0.4550	6.975	0.784	0.4650	5.050	0.866	0.3367
F1*F5	–0.875	0.843	–0.0088	–1.625	0.784	–0.01625	–0.425	0.866	–0.00425
F1*F9	0.250	0.843	0.00083	–0.950	0.784	–0.00317	–2.075	0.866	–0.00692
F4*F5	–0.425	0.843	–0.00113	–0.025	0.784	–0.00007	–1.525	0.866	–0.00407
F4*F9	0.700	0.843	0.00062	–0.000	0.784	0.00000	1.025	0.866	0.000911
F5*F9	–0.800	0.843	–0.00011	–0.925	0.784	–0.000123	–0.400	0.866	–0.000053

[a] Coefficient

[b] Standard error of coefficient

R-squared (R^2) is a statistical measure and some information is given about the appropriateness of regression equation with response variables. The obtained equation is better fitted with the response when R^2 value increases and is close to one. Adjusted R^2 is a modification and better than R^2 because R^2would always increase by adding a new predictor and some of this increase is due to chance and not because the model is a better fit. The adjusted R2, however, changes only when the independent variables are really influenced by the dependent variables and increases when the model is improved with a new predictor more than expected by chance [25]. The adjusted R^2values are 90.97, 93.54, and 91.36 for extraction of MRT, DMR, and 8-OHD, respectively, and indicate the polynomial model equation fits well to response variables at the 95 % confidence level.

The lack of fit (LOF) is an important component in the ANOVA Table which displays whether the model fits into the data well. For this propose, a lack of fit F-test is used

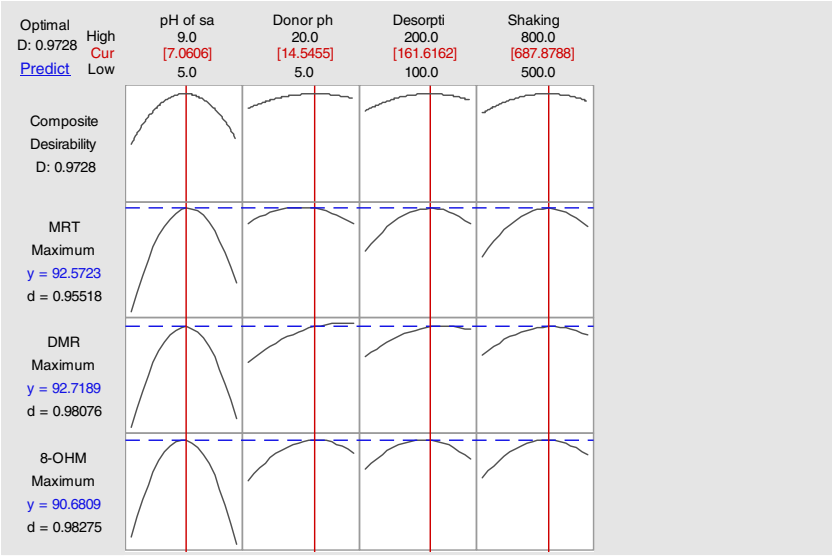

Fig. 5 Optimization plot Profiles MRT, DMR and 8-OHM for predicated values for ER%

Table 4 Effect of SPME sorbents on the extraction recovery percentage of MRT, DMR, and 8-OHD ($n = 3$)

SPME sorbent	Analytes	MRT		DMR		8-OHD	
	Concentration (ng mL^{-1})	25	75	25	75	25	75
MGO	Found (ng mL^{-1})	15.42 ± 0.09	44.56 ± 0.08	14.43 ± 0.09	47.47 ± 0.09	18.14 ± 0.09	55.69 ± 0.09
	Recovery percentage	61.7	59.4	57.7	63.3	72.6	74.2
MGOPA	Found (ng mL^{-1})	22.54 ± 0.06	69.02 ± 0.06	22.79 ± 0.08	69.45 ± 0.06	22.67 ± 0.07	82.13 ± 0.08
	Recovery percentage	90.2	92.0	91.2	92.6	90.7	109.5

and F-value is obtained by dividing the mean square lack of fit to the mean square of pure error. According to the F-test, if the *p*-value of LOF is high and larger than the selected α-level, the null hypothesis is not rejected and indicates that the model is a good fit to the responses. The *p*-values for the lack of fit test were 0.271, 0.101, and 0.225 for extraction of MRT, DMR, and 8-OHD, respectively. As the *p*-values are higher than the α-level (0.05), these models are well fitted to the data.

The regression coefficients in uncoded units (Table 3) show that the pH is the most significant compared to other factors. The regression coefficients show positive values for three main factors, desorption time, pH of sample solution, and shaking rate and negative for donor phase volume. Comparison of interaction between the two similar main factors shows that the effect of pH is larger than three other factors and has a negative value. The results also indicate that the interaction between the pH of sample solution and donor phase volume is more significant than to interaction between other main factors, and the interaction between desorption time and shaking rate is minimally effective.

After obtaining the fitted model for extraction of MRT, DMR, and 8-OHD, the optimization plot (Fig. 5) can be used to predict the effect of change of each factor on the responses and composite desirability of response. The optimization plot for extraction of MRT, DMR, and 8-OHM is shown in Fig. 5. In order to obtain an optimization plot, the maximum response is selected as the goal. Figure 5 indicates that the maximum responses are 92.5723, 92.7189, and 90.6809, with a desirability of 0.95518, 0.98076, and 0.98275 for extraction of MRT, DMR, and 8-OHD, respectively. Based on Fig. 5, the experimental conditions for significant factors are chosen: pH, 7.1; donor phase volume, 14.5 (mL); desorption time, 162 s; shaking rate, ~700 (rpm).

Comparison of the magnetic graphene oxide–polyaniline nanocomposite with magnetic graphene oxide nanocomposite as SPME sorbent

The magnetic graphene oxide nanocomposite was prepared by the method described above with the exception that graphene oxide (0.2 g) was used instead of graphene oxide–polyaniline and applied for extraction of MRT, DMR, and 8-OHM based on the method above (Table 4). The results indicate that the MGOPN provides higher extraction recovery than MGO and is quite effective as SPME sorbent for extraction of all analytes. It seems that the most important parameter in this phenomenon is the type and strength of the interaction between the analyte and sorbent surface. In the MGOPN, strong inter-molecular forces are formed between the delocalized π-electron on MGOPN with the aromatic heterocyclic ring in the analytes, Therefore, due to this strong interaction between SPME sorbent and analytes, the ER% is high.

The MGO has hydroxyl groups on its surface, which can easily form hydrogen bonds with suitable functional groups in the analytes. Nitrogen atoms in the heterocyclic ring of the analytes can form hydrogen bonds with MGO, but due to the space congestion and exposure to nitrogen atoms in the aromatic heterocyclic ring, this interaction is weak and so ER% is low. The results also show that the ER% of 8-OHM with MGO is higher than the ER% of MRT and DMR because strong hydrogen bonds are formed between the hydroxyl group of between 8-OHM with MGO.

Method validation

In order to investigate the practical applicability of the proposed method for the determination of MRT, DMR, and 8-

Table 5 Linearity, repeatability, detection limits, and preconcentration factor of the proposed analytical procedure

Analyte	linear dynamic range (ngmL^{-1})	R^2	LOD (ngmL^{-1})	LOQ (ngmL^{-1})	RSD% ($n = 5$)		Preconcentration factor
					Intraday	Interday	
MRT	0.9–450	0.9967	0.4	0.9	5.9	9.3	158
DMR	3.0–500	0.9921	1.1	3.0	6.6	9.8	109
8-OHD	1.4–500	0.9935	0.5	1.4	6.3	10.1	124

OHM, several parameters such as linear dynamic range, limit of detection, limit of quantification, and relative standard deviations (RSD%) were evaluated under the optimum conditions and summarized in Table 5. The preconcentration factor was calculated using the equation stated above and were 158, 109, and 124 for extraction of MRT, DMR, and 8-OHM by the proposed method, respectively.

The method was linear over the concentration range 0.9–450, 3.0–500, and 1.4–500 ngmL^{-1} with the coefficient of determination, r^2, higher than 0.9921 for MRT, DMR, and 8-OHM, respectively. The limit of detection (LOD) for extraction of MRT, DMR, and 8-OHM were 0.4, 1.1, and 0.5 ngmL^{-1}, respectively, and limit of quantitation (LOQ) was less than 3.0 ngmL^{-1} for all analytes.

The precision of the method was evaluated with five replicate experiments for the spiked samples with 20 ng mL^{-1}of MRT, DMR, and 8-OHM on the same day and on three consecutive days. The intra-day and inter-day relative standard deviations were less than 6.6 and 10.1 ($n = 5$), respectively, indicating the proposed method has a suitable reproducibility and precision for analysis of MRT, DMR, and 8-OHM (Table 5).

Real samples analysis

The proposed method was finally employed for determination of MRT and its metabolites in several real water and human urine samples. Each experiment was carried out for three replicates and the mean extraction recoveries were used as responses. Drug-free human urine samples were obtained from healthy volunteers. Post-dose human urine samples were taken from healthy volunteers after a single oral administration of 45 mg of MRT (Remeron, N.V. Organon) after 20–28 h, and stored in polypropylene tubes at 20 °C. Well water and river water samples were obtained from the outskirts of Mashhad and Golestan River (Mashhad, Iran), respectively. All real samples were centrifuged at 8000 rpm for 5 min and filtered to remove any solid particles. In order to evaluate the matrix effect, all the drug-free human urine and real water samples were centrifuged at 8000 rpm for 5 min and spiked at two different concentrations (20 and 50 ngmL^{-1}) of MRT, DMR, and 8-OHM. The mean extraction recoveries for extraction of MRT, DMR, and 8-OHM are summarized in Table 6. The obtained relative recoveries are between 80.3 and 119.8 %, indicating that the matrix effects are minimal. These results demonstrate that the proposed procedure can be successfully applied to the analysis of MRT, DMR, and 8-OHM in real samples such as human urine and water samples. Figure 6 shows the chromatogram of human urine samples from healthy volunteers spiked with 20 ng mL^{-1} of MRT, DMR, and 8-OHM. The results also indicate that no significant interfering peaks are observed in the region of interest where the analytes are eluted for all the real samples.

Table 6 Assay of MRT and its metabolites in real water and human urine samples by means of the proposed method ($n = 3$)

Analytes		MRT			DMR			8-OHM		
Spiked value (ng mL^{-1})		0	20	50	0	20	50	0	20	50
Well water	Found (ng mL^{-1})	Nd	17.92 ± 0.07	45.04 ± 0.06	Nd	23.96 ± 0.08	42.31 ± 0.07	Nd	17.55 ± 0.08	43.14 ± 0.07
	Recovery percentage	–	89.6	90.1	–	119.8	84.6	–	87.8	86.3
River water	Found(ng mL^{-1})	Nd	16.83 ± 0.07	42.71 ± 0.07	Nd	16.35 ± 0.07	41.15 ± 0.08	Nd	17.23 ± 0.09	43.34 ± 0.09
	Recovery percentage	–	84.2	85.4	–	81.8	82.3	–	86.2	86.7
Human urine	Found(ng mL^{-1})	Nd	16.05 ± 0.09	40.15 ± 0.09	Nd	16.19 ± 0.08	40.85 ± 0.09	Nd	16.71 ± 0.09	41.21 ± 0.09
	Recovery percentage	–	80.2	80.3	–	80.9	81.2	–	83.6	82.4
Infected human urine	Found(ng mL^{-1})	10.3 ± 0.2	–	–	18.7 ± 0.2	–	–	39.2 ± 0.2	–	–

Nd not detected

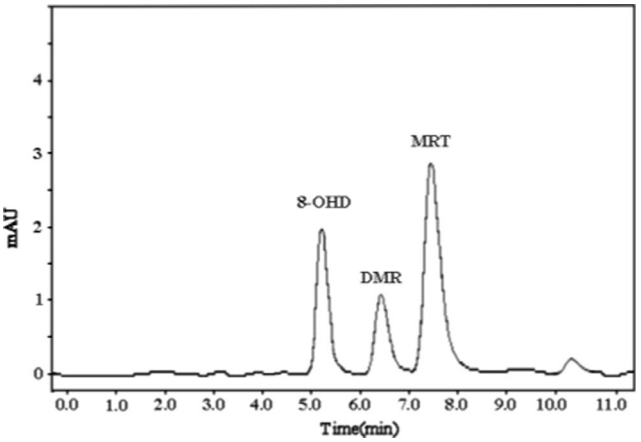

Fig. 6 Chromatogram of spiked human urine sample at 20 $ngmL^{1-}$ for MRT, DMR, and 8-OHM under optimum conditions

Conclusions

An inexpensive, new, simple, and rapid UAMDSPME method was described for extraction of MRT and its metabolites from real water and human urine samples. The magnetic graphene oxide–polyaniline nanocomposite was prepared and applied as a new sorbent for UAMDSPME. The new sorbent showed high preconcentration factor and selectivity for these analytes. A multivariate strategy based on two steps, P-B design and B-B design, was used for screening and optimizing the main effecting factors for extraction of MRT, DMR, and 8-OHM by UAMDSPME. The proposed microextraction method shows several advantages, including low extraction time, simple operation, cost effectiveness, is rapid, is organic solvent free, has high preconcentration factor, low sorbent consumption, and variety in the choice of sorbent [4]. Morevore, The resulting optimized procedure could be potentially applied for determination of MRT, DMR, and 8-OHM using UAMDSPME combined with HPLC. The application of the method to real samples demonstrated that this procedure is suitable and capable for quantitative analysis of MRT, DMR, and 8-OHM in real water and biological samples for routine laboratories analysis.

Acknowledgments The authors gratefully acknowledge support of this research by the Ferdowsi University of Mashhad, Mashhad, Iran (no.3/32789 dated 12/21/2014).

Compliance with ethical standards

Conflict of interest The authors declare no conflict of interest.

The study has been carried out in accordance with the ethical standards of the institutional and/or national research committee and with the 1964 Helsinki declaration and its later amendments or comparable ethical standards.

The human urine samples were collected from voluntary donors with their informed consent.

References

1. Brooks BW, Chambliss CK, Stanley JK, Ramirez A, Banks KE, Johnson RD, et al. Determination of select antidepressants in fish from an effluent-dominated stream. Environ Toxicol Chem. 2005;24(2):464–9.
2. Stanley JK, Ramirez AJ, Chambliss CK, Brooks BW. Enantiospecific sublethal effects of the antidepressant fluoxetine to a model aquatic vertebrate and invertebrate. Chemosphere. 2007;69(1):9–16.
3. Alawi M, Alahmad W. Simultaneous determination of some pharmaceuticals in hospital effluents using HPLC with UV and fluorescence detectors. Jordan J Pharm Sci. 2012;5(1).
4. Ghorbani M, Chamsaz M, Rounaghi GH. Ultrasound-assisted magnetic dispersive solid-phase microextraction: a novel approach for the rapid and efficient microextraction of naproxen and ibuprofen employing experimental design with high-performance liquid chromatography. J Sep Sci. 2016;39(6):1082–9.
5. Giorgi M, Yun H. Pharmacokinetics of mirtazapine and its main metabolites in Beagle dogs: a pilot study. Vet J. 2012;192(2):239–41.
6. Timmer CJ, Sitsen JA, Delbressine LP. Clinical pharmacokinetics of mirtazapine. Clin Pharmacokinet. 2000;38(6):461–74.
7. Timmer C, Paanakker J, Van Hal H. Pharmacokinetics of mirtazapine from orally administered tablets: influence of gender, age, and treatment regimen. Hum Psychopharm Clin. 1996;11(6):497–509.
8. Brockmöller J, Meineke I, Kirchheiner J. Pharmacokinetics of mirtazapine: enantioselective effects of the CYP2D6 ultra rapid metabolizer genotype and correlation with adverse effects. Clin Pharmacol Ther. 2007;81(5):699–707.
9. Enggaard TP, Mikkelsen SS, Zwisler ST, Klitgaard NA, Sindrup SH. The effects of gabapentin in human experimental pain models. Scand J Pain. 2010;1(3):143–8.
10. Deng H, Teo AKL, Gao Z. An interference-free glucose biosensor based on a novel low potential redox polymer mediator. Sensor Actuat B Chem. 2014;191:522–8.
11. Allafchian AR, Majidian Z, Ielbeigi V, Tabrizchi M. A novel method for the determination of three volatile organic compounds in exhaled breath by solid-phase microextraction–ion mobility spectrometry. Anal Bioanal Chem. 2016;408(3):839–47.
12. Saraji M, Jafari MT, Sherafatmand H. Sol–gel/nanoclay composite as a solid-phase microextraction fiber coating for the determination of organophosphorus pesticides in water samples. Anal Bioanal Chem. 2015;407(4):1241–52.
13. Feng J, Sun M, Bu Y, Luo C. Development of a functionalized polymeric ionic liquid monolith for solid-phase microextraction of polar endocrine disrupting chemicals in aqueous samples coupled to high-performance liquid chromatography. Anal Bioanal Chem. 2015;407(23):7025–35.
14. Ghorbani M, Chamsaz M, Rounaghi GH. Glycine functionalized multiwall carbon nanotubes as a novel hollow fiber solid-phase microextraction sorbent for preconcentration of venlafaxine and o-desmethylvenlafaxine in biological and water samples prior to determination by high-performance liquid chromatography. Anal Bioanal Chem. 2016;408(16):4247–56.
15. Mahpishanian S, Sereshti H. Graphene oxide-based dispersive micro-solid phase extraction for separation and preconcentration of nicotine from biological and environmental water samples followed by gas chromatography-flame ionization detection. Talanta. 2014;130:71–7.
16. Daneshvar Tarigh G, Shemirani F. Development of a selective and pH-independent method for the analysis of ultra trace amounts of nitrite in environmental water samples after dispersive magnetic

solid phase extraction by spectrofluorimetry. Talanta. 2014;128: 354–9.
17. Wen Y, Niu Z, Ma Y, Ma J, Chen L. Graphene oxide-based microspheres for the dispersive solid-phase extraction of non-steroidal estrogens from water samples. J Chromatogr A. 2014;1368:18–25.
18. Xue X, Yang D, Wang D, Xu X, Zhu L, Zhao Z. Solidification of floating organic drop liquid-phase microextraction cell fishing with gas chromatography–mass spectrometry for screening bioactive components from *Amomum villosum* Lour. Biomed Chromatogr. 2015;29(4):626–32.
19. Du D, Wang L, Shao Y, Wang J, Engelhard MH, Lin Y. Functionalized graphene oxide as a nanocarrier in a multienzyme labeling amplification strategy for ultrasensitive electrochemical immunoassay of phosphorylated p53 (S392). Anal Chem. 2011;83(3):746–52.
20. Liu Y, Deng R, Wang Z, Liu H. Carboxyl-functionalized graphene oxide–polyaniline composite as a promising supercapacitor material. J Mater Chem. 2012;22(27):13619–24.
21. Abedi H, Ebrahimzadeh H. Electromembrane-surrounded solid-phase microextraction coupled to ion mobility spectrometry for the determination of nonsteroidal anti-inflammatory drugs: a rapid screening method in complicated matrices. J Sep Sci. 2015;38(8): 1358–64.
22. Ebrahimzadeh H, Yamini Y, Kamarei F. Optimization of dispersive liquid–liquid microextraction combined with gas chromatography for the analysis of nitroaromatic compounds in water. Talanta. 2009;79(5):1472–7.
23. Zhang J, Liang Z, Li S, Li Y, Peng B, Zhou W, et al. In-situ metathesis reaction combined with ultrasound-assisted ionic liquid dispersive liquid–liquid microextraction method for the determination of phenylurea pesticides in water samples. Talanta. 2012;98: 145–51.
24. Ferreira SC, Bruns R, Ferreira H, Matos G, David J, Brandao G, et al. Box-Behnken design: an alternative for the optimization of analytical methods. Anal Chim Acta. 2007;597(2):179–86.
25. Khodadoust S, Ghaedi M, Hadjmohammadi M. Dispersive nano solid material-ultrasound assisted microextraction as a novel method for extraction and determination of bendiocarb and promecarb: response surface methodology. Talanta. 2013;116:637–46.